crystals

MDPI

Article

Experimental Investigation and Image Processing to Predict the Properties of Concrete with the Addition of Nano Silica and Rice Husk Ash

Siva Avudaiappan [1,*], Supriya Prakatanoju [2], Mugahed Amran [3,4,*], Radhamanohar Aepuru [5], Erick I. Saavedra Flores [1], Raj Das [6], Rishi Gupta [7], Roman Fediuk [8] and Nikolai Vatin [9]

1 Departamento de Ingeniería en Obras Civiles, Universidad de Santiago de Chile, Av. Ecuador 3659, Estación Central 9160000, Chile; erick.saavedra@usach.cl
2 Department of Civil Engineering, Vaagdevi College of Engineering, Warangal 506005, India; supriyaprakatanoju807@gmail.com
3 Department of Civil Engineering, College of Engineering, Prince Sattam Bin Abdulaziz University, Alkharj 16273, Saudi Arabia
4 Department of Civil Engineering, Faculty of Engineering, Amran University and IT, Quhal 9677, Amran Province, Yemen
5 Departamento de Ingeniería Mecánica, Facultad de Ingeniería, Universidad Tecnologica Metropolitana, Dieciocho 161, Santiago 8330378, Chile; raepuru@utem.cl
6 School of Engineering, RMIT University, 124 La Trobe Street, Melbourne, VIC 3000, Australia; raj.das@rmit.edu.au
7 Department of Civil Engineering, University of British Columbia, Vancouver, BC V6T 1Z4, Canada; guptar@uvic.ca
8 Polytechnic Institute, Far Eastern Federal University, Sukhanova Str., 690922 Vladivostok, Russia; roman44@yandex.ru
9 Peter the Great St. Petersburg Polytechnic University, 195251 St. Petersburg, Russia; vatin@mail.ru
* Correspondence: siva.avudaiappan@usach.cl (S.A.); m.amran@psau.edu.sa or mugahed_amran@hotmail.com (M.A.)

check for updates

Citation: Avudaiappan, S.; Prakatanoju, S.; Amran, M.; Aepuru, R.; Saavedra Flores, E.I.; Das, R.; Gupta, R.; Fediuk, R.; Vatin, N. Experimental Investigation and Image Processing to Predict the Properties of Concrete with the Addition of Nano Silica and Rice Husk Ash. *Crystals* **2021**, *11*, 1230. https://doi.org/10.3390/cryst11101230

Academic Editors: Yurii Barabanshchikov and Chongchong Qi

Received: 24 August 2021
Accepted: 5 October 2021
Published: 12 October 2021

Publisher's Note: MDPI stays neutral with regard to jurisdictional claims in published maps and institutional affiliations.

Copyright: © 2021 by the authors. Licensee MDPI, Basel, Switzerland. This article is an open access article distributed under the terms and conditions of the Creative Commons Attribution (CC BY) license (https://creativecommons.org/licenses/by/4.0/).

Abstract: The use of the combination of ultrafine rice husk ash (RHA) and nano silica (NS) enhances the compactness of hardened concrete, but there is still a lack of studies that address the effects of NS and RHA on the workability, mechanical properties and pore microstructure of concrete. This study mainly aims to investigate the influence of the pore size distribution in multiphysics concrete model modified by NS and RHA and to determine the workability and mechanical properties of concrete with NS and RHA. In this work, NS and RHA were used as 0, 5, 10, 15 and 20% replacements of ordinary Portland cement (OPC) in concrete grade M20. Concrete mixed with NS and RHA showed improved performance for up to 10% addition of NS and RHA. Further addition of NS and RHA showed a decrease in performance at 7, 14 and 28 days. The decrease in concrete porosity was also found to be up to 10% when adding NS and RHA to cement. Image processing was performed on the cement-based materials to describe the microstructure of the targeted material without damage. The results from the experimental and tomography images were utilized to investigate the concrete microstructure and predict its inner properties.

Keywords: image processing; nano silica; rice husk ash; pore microstructure; multiphysics concrete model; properties

1. Introduction

NS is manufactured using thermo-decomposition, sol-gel of silica fume and vapor-phase reaction. It is used in several applications such as ceramics, chemicals/catalysis analysis, and biological science [1]. NS is synthesized using chemicals that control the shape, size, and purity of the materials. RHA is an agricultural by-product that contains a high amount of silica. In recent years, the construction industry has attempted to

incorporate NS and RHA in the production of concrete to reduce the cost of the structure [2]. Conventional concrete is mainly composed of cement, coarse aggregate, fine aggregate, and an adequate amount of water. The rapid growth in the construction industry and the vast formation of waste have pushed the development of sustainable products using RHA, micronized biomass silica, ground granulated blast-furnace slag, crumbed rubber, NS, different fibers, superplasticizers, and different admixtures, among others, in conjunction with concrete [3]. In general, the use of admixtures, minerals, or artificial waste materials can provide sustainable concrete with moderate cost and several benefits in terms of avoiding environmental pollution by effectively disposing of waste or by-products, which could pollute lands, water, and air to a large extent [4]. In this investigation, RHA and NS are considered waste, which could potentially be used to partially replace fine aggregate to improve concrete strength.

After a comprehensive survey, it was observed that the addition of RHA to concrete or mortar increased their durability, compressive strength, workability and flexural strength [5]. It was also found that incorporating NS with RHA dramatically decreases the compressive strength at an early age but increases at a later age. NS increases the heat of hydration of concrete or mortar and hardens the cement paste by forming calcium silicate hydrate (C-S-H). The optimum use of RHA with NS enhances the chloride permeability, electrical resistivity, and capillary absorption in concrete mixes or mortar [6]. The colloidal NS decreases the workability of concrete but increases its compressive and tensile strength compared to the nominal mix. It was also found that a high dosage of RHA decreases the strength with the addition of NS in concrete. Ultrafine RHA of particle size between 5 and 95 μm increases the strength but reduces water absorption capacity in concrete [7]. NS distributes uniformly in concrete with higher water permeability resistance, which is identified from the microstructural analyses [8]. An optimum dose of 30% of RHA unfavorably influences concrete workability, strength, and water permeability [9]. The use of ultrafine RHA enhances the compactness of concrete. An optimum dosage increased the workability of concrete with RHA and its compressive strength was improved by adding NS [10].

The 2D X-ray image processing techniques are performed using a linear traverse for predicting air-voids. The high accuracy of 3D is used to predict the distribution of air-voids in the hardened concrete. Thus, the pore microstructure of concrete without damage was investigated by means of a non-destructive method. We note that X-ray imaging techniques have been previously used to characterize pore microstructure and compressive strength of cement-based materials and organic foams [11,12]. However, there is a lack of investigating the effect of NS and RHA on the workability, mechanical properties, and pore microstructure of concrete. In particular, this study focuses on the determination of the optimum dosage of RHA and NS. We also compare the properties of conventional concrete with RHA and NS concrete. Our main interest is to develop sustainable concrete with the use of RHA and NS. Therefore, the investigation of the influence of NS and RHA on concrete, with the aid of image processing, will help to understand their combined properties and microstructure. The inclusion of RHA as a partial replacement of cement shows significant pozzolanic and filler effects on the mechanical properties and microstructure of concrete [13,14]. The porosity of the resulting samples was shown to be the most important element influencing concrete strength qualities; nevertheless, pores with radii less than 10 nm had only a minor impact on the final strength [15]. The strength of the equivalent porosities increased as the amount of hydrate phases increased. There is no considerable effect on strength due to the specific surface area. The increasing water-to-cement ratio and sand-to-cement ratio increased the probable pore size and threshold radius. In addition, existing multiphysics models of pore size distribution in cement-based materials were examined and compared to the test results [16]. Finally, the extended Bhattacharjee model was built to examine the relationship between compressive strength and pore structure. A novel multiphysics empirical model was proposed to relate the in situ strength of concrete

to its porosity, pore size characteristics, cement concentration, aggregate type, exposure conditions, and other factors [17].

2. Experimental Program

2.1. Materials

Dalmia cement of 53 Grade OPC according to IS: 269-2015 was used for this study. Agricultural waste or by-product RHA and NS was commercially purchased in Tamilnadu, India. The NS product is organic and has super-pozzolana with high silica content with a particle size of 25 µm mostly. RHA was manufactured by controlled burning the agriculture waste such as rice husk in between 600 and 700 °C. NS is a fluffy white powder made up of amorphous silica powder of high purity, which is procured from Astra Chemicals. The physical and chemical characteristics of RHA and NS are given in Tables 1 and 2, respectively. The fine natural aggregate conforming to zone II and coarse aggregate of maximum 20 mm size according to IS: 383-2016, IS: 2386-1 and IS: 2386 was used in this study. As per Indian Standards, the portable water free from impurities available in the laboratory was used for mixing and curing purposes. The physical and chemical properties of NS are shown in Table 1, and the chemical composition of RHA is shown in Tables 2 and 3.

Table 1. Physical and chemical properties of NS.

Description	Values	Chemical Composition	Contents (%)
Particle size (µm)	15–20	Silicon dioxide (SiO_2)	94.3
Surface area (m^2/g)	640	Aluminium oxide(Al_2O_3)	0.06
Bulk density (g/cm^3)	0.08–0.10	Ferric oxide (Fe_2O_3)	0.46
Molecule	SiO_2	Calcium oxide (CaO)	0.51
Molecular weight	60.08	Titanium dioxide (TiO_2)	2.31
Porosity (mL/g)	0.6	Loss of Ignition	2.25
Morphology	Porous and spherical	-	-

Table 2. Physical composition of RHA.

Physical Properties	Values
Microscopic Investigation	Crystalline Structure
Burning Temperature	400–700 °C
Grinding Time	90 min
Fineness	Passing 200–325 µ Sieves
Specific Gravity	2.14

Table 3. Chemical composition of RHA.

Chemical Properties	Value (%)
Silicon dioxide (SiO_2)	88.32
Aluminium oxide (Al_2O_3)	0.46
Ferric oxide (Fe_2O_3)	0.67
Calcium oxide (CaO)	0.51
Magnesium oxide (MgO)	0.44
Sodium Oxide (Na_2O)	0.12
Potassium Oxide (K_2O)	2.91

2.2. Mix Design and Mixing Procedure

Indian Standard IS: 10262-2009 procedure was adopted for the mix design of M20 concrete grade. Based on the water–cement ratio, the workability of concrete is adjusted for each trial. Super-plasticizer is prepared separately prior to mixing with a dry mix of fine aggregates, coarse aggregates, cement, RHA, and NS (Figure 1). The solution of water and

polycarboxylate super-plasticizer, which was procured from Astra Chemicals, was added to the dry mix in the mixer, and mixing was continued until the materials were distributed uniformly. The mixing was carried out at the atmospheric temperature of 27 ± 2 °C for half an hour from the time of addition of water to the dry ingredients with 90% relative humidity until the experiment was completed.

Figure 1. Materials, mix design and mixing procedure.

After the concrete was mixed, the standard cube mold of the size of 150 × 150 × 150 mm^3, a cylindrical mold of 200 mm height and 100 mm diameter, and a prism mold of size 500 × 100 × 100 mm^3 were immediately filled with concrete and placed for vibration until concrete was compacted. Concrete specimens were cast with different ratios of RHA and NS. The obtained NS was added to improve the performance of concrete, because NS contains pozzolanic reacting to blended concrete, besides the pore-filling effects in concrete. The incorporation of nano silica increases the compressive strength of concrete with optimum usage of nano silica up to 2% with 15–80 nm particle size. The ambient temperature conditions were maintained, and specimens were kept free from vibration. After 24 hr, the specimens were removed from molds and submerged immediately into water until testing. Depending on the tests, specimens were cured in clear water for 3, 7, and 28 days, respectively.

2.3. Testing

In this experimental work, the properties of fresh and hardened concrete mixes were measured according to the Indian Standards IS: 1199-1959, IS: 516-1959, and IS: 55816-1999. Compaction factor and slump cone test comprise the workability test for concrete. Fresh concrete workability with various proportions of NS at 0, 0.5, 1.0, 1.5, and 2.0% and RHA combined at 0, 5, 10, 15, and 20% by weight of cement was assessed by slump cone testing and compaction factor testing, as shown in Figure 2. Hardened concrete specimens were tested for compressive strength, split-tensile strength, and flexural strength at 3, 7, and 28 days, respectively, as shown in Figure 3.

Figure 2. Fresh concrete tests: (**a**) Compaction factor test and (**b**) Slump cone test.

Figure 3. Hardened Concrete tests: (**a**) Compressive strength test, (**b**) Flexural strength test and (**c**) Split tensile strength test.

2.4. Workability

Slump refers to the average diameter of the concrete after the typical slump cone has been released, and it is one of the most essential indicators for determining concrete plasticizing performance [13]. The slump cone test is a very critical test for evaluating concrete workability. Concrete slump cone testing was conducted for different amounts of NS and RHA. The slump cone results of NS and RHA with different ratios are shown in Table 4. Nano-silica modified concrete has a slump value which is 40–60% lower than that of ordinary concrete, according to Björnström and Quercia et al. [14,15]. During the slump test, a tiny amount of water was found leaking from the fresh concrete [16,17]. Because of its high specific surface area and the huge number of unsaturated bonds, NS has a super-high reaction capacity when it replaces cement. This makes it easier to attract nearby water molecules to form chemical bonds. As a result, there is no water segregation or exudation from the nano-silica mixture [18–20]. Because silica particles have a higher specific surface area than cement, they absorb more water and lessen the slump of concrete, according to Beigi et al. [21].

Table 4. Slump cone test results.

No. of Sample	NS and RHA in Concrete (%)	Slump Value (mm)
1	0%	75
2	0.5% NS & 5% RHA	70
3	1.0% NS & 10% RHA	65
4	1.5% NS & 15% RHA	60
5	2.0% NS & 20% RHA	55

The compaction factor test was performed to determine the degree of compaction of concrete. The compaction factor test was carried out using the Slump Cone Test for different replacement levels of NS and RHA. Table 5 shows the compaction factor results obtained using NS and RHA. The additions of NS and RHA to M20 grade concrete were improved workability up to 10%. With a higher percentage of NS and RHA, workability was lower due to the higher water absorption rate of NS and RHA.

Table 5. Compaction factor test results.

No. of Sample	NS and RHA in Concrete (%)	Slump Value (mm)
1	0%	0.90
2	0.5% NS & 5% RHA	0.88
3	1.0% NS & 10% RHA	0.86
4	1.5% NS & 15% RHA	0.85
5	2.0% NS & 20% RHA	0.83

3. Results and Discussions

3.1. Compressive Strength

The compression test was conducted using a compression testing cm^3. Cube specimens were 15 cm in size. Aggregate size did not exceed 20 mm. For different replacement levels of NS and RHA, the compressive strength of all the mixes were determined at the ages of 7, 14, and 28 days. For traditional categories, three samples were measured, and the mean compressive strength of the three samples was considered to be the compressive strength of the specified category. Table 6 and Figure 3 show the compressive strength test results. Figure 4 shows a comparison of the compressive strength of concrete with different proportions of NS and RHA. Here we can observe that the addition of NS and RHA increased the compressive strength for 28 days up to 10% and decreased at further increase. The pozzolanic reaction between nano silica and calcium hydroxide, which promotes the development of hydrated calcium silicate, is the fundamental reason for the increase in concrete compressive strength.

Table 6. Compressive strength of concrete.

No. of Sample	NS and RHA in Concrete (%)	Compressive Strength (N/mm^2)		
		7 Days	14 Days	28 Days
1	0%	17.8	20.7	24.5
2	0.5% NS & 5% RHA	18.3	23.1	27.3
3	1.0% NS & 10% RHA	19.9	26.2	31.3
4	1.5% NS & 15% RHA	19.1	25.5	30.7
5	2.0% NS & 20% RHA	18.6	22.8	26.1

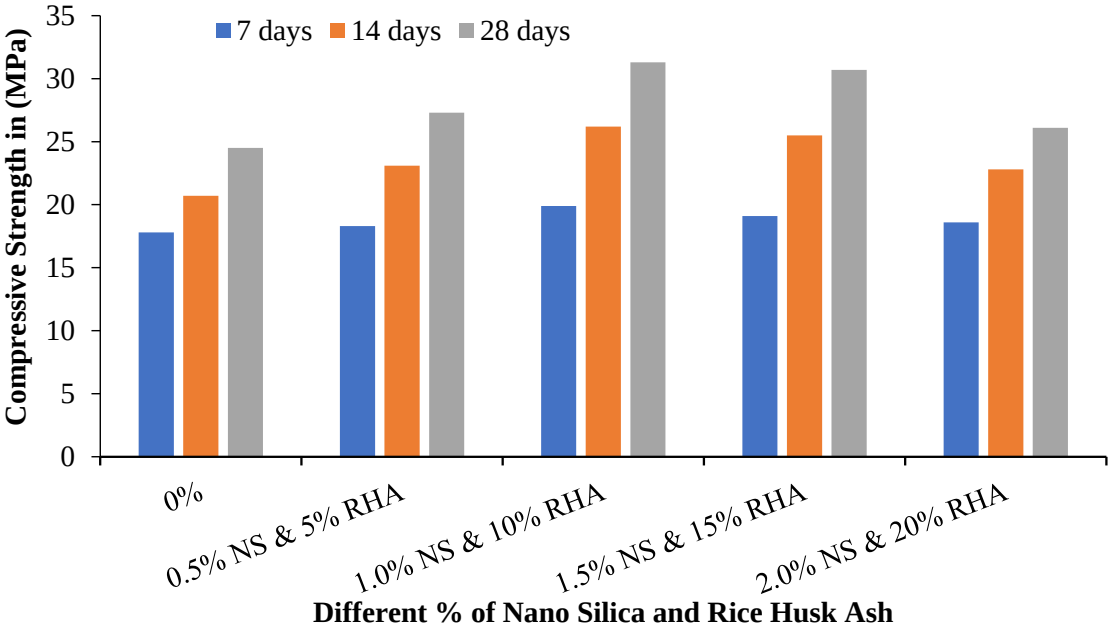

Figure 4. Comparison of compressive strength of concrete with different proportions of NS and RHA.

On the other hand, concrete without NS can only hydrate to a minimum of calcium silicate hydrate by relying on cement. One of the essential components that contribute to strength is hydrated calcium silicate. As a result, concrete without NS has a low compressive strength [22,23]. Jalal and Abdellahi et al. [24,25] discovered that the early strength improvement effect of nano-silica modified concrete is more prominent due to the greater pozzolan activity of nano-silica particles [26–29]. In natural pozzolan-based polymers, nanosilica not only speeds up the polymerization reaction, but also encourages

the formation of calcium silicate hydrates (C-S-H) and sodium aluminosilicate hydrates (N-A-S-H) [30].

3.2. Flexural Strength

In these experiments, a prism size of 150 × 150 × 700 mm^3 was used. For different replacement levels of NS and RHA, the flexural strength of all the mixes was determined at the ages of 7, 14, and 28 days [31]. Table 7 and Figure 5 show the flexural strength of concrete test results. Figure 4 shows the flexural strength of concrete with different proportions of NS and RHA. The addition of NS and RHA improved the flexural strength at 28 days for a NS and RHA content up to 10%. The flexural strength of NS concrete similarly varies in comparison with the compressive strength. The flexural strength of the mortar increased when the NS concentration was increased from 3% to 10%, according to Ltifiy et al. [31]. When the nano-SiO concentration was 6–10%, Rong et al. [32] discovered that the nano silica concrete offered the highest flexural strength after curing of 3 days, 7 days, 28 days, and 90 days. Huu-Bang Tran et al.'s experimental results show that the strengths significantly increased when NS content increased from 0 to 1.5%; however, the strength decreased with a further increase in NS content [33]. Thus, the appropriate NS content was to be found close to 1.5%. These results were similar to the previous findings reported by many researchers worldwide [34–46].

Table 7. Flexural strength of concrete.

No. of Sample	NS and RHA in Concrete (%)	Compressive Strength (N/mm^2)		
		7 Days	14 Days	28 Days
1	0%	3.16	3.412	3.71
2	0.5% NS & 5% RHA	3.21	3.60	3.91
3	1.0% NS & 10% RHA	3.34	3.842	4.2
4	1.5% NS &15% RHA	3.28	3.789	4.15
5	2.0% NS & 20% RHA	3.23	3.58	3.83

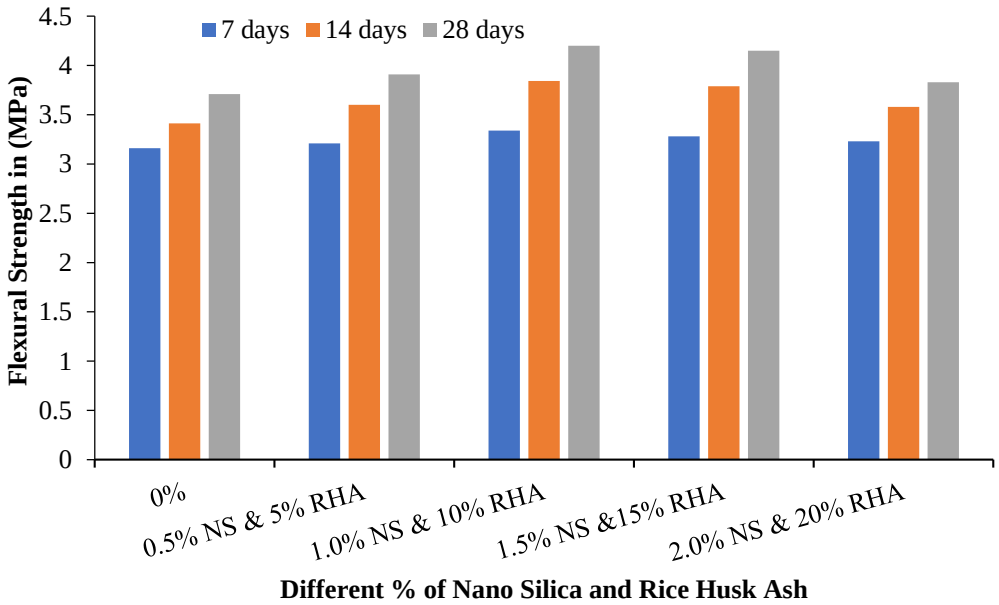

Figure 5. Comparison of flexural strength of concrete with different proportions of NS and RHA.

3.3. Split Tensile Strength

In these experiments, cylindrical specimens of 30 cm height and 15 cm diameter were considered. For different replacement levels of NS and RHA, all the mixes' split tensile strength was determined at the ages of 7, 14, and 28 days. Table 8 and Figure 5 show the

split tensile strength test results. Figure 6 shows the split tensile strength of concrete with different content of NS and RHA. The addition of NS and RHA resulted in an increase of the split tensile strength at 28 days. This trend was observed up to 10% for all NS and RHA content mechanical properties, which can be explained by the rapid consumption of calcium hydroxide produced during the hydration process. After 10% NS and RHA content, the reduced concrete strength values can be attributed to the proportions of NS and RHA, which are higher than the amount needed during the hydration process to be combined with the released lime. Redaelli et al. [10] tested the splitting tensile strength of nano-SiO concrete. When 3% nano-SiO replaced cement, the tensile strength of NS modified concrete was improved by 16.10% over that of ordinary concrete. Fallah et al. [33] tested the splitting tensile strength of nano-SiO concrete. When 8% nano-SiO replaced cement, the tensile strength of NS modified concrete was improved by 16.10% over that of ordinary concrete. Nano-SiO enhances the interfacial strength between the concrete matrix and the aggregate, which causes this behavior [21]. The addition of nano-SiO to concrete serves as both a nano-reinforcement and a filling agent, filling the holes in the concrete matrix [34].

Table 8. Split tensile strength of concrete.

No. of Sample	NS and RHA in Concrete (%)	Compressive Strength (N/mm^2)		
		7 Days	14 Days	28 Days
1	0%	1.98	2.32	2.56
2	0.5% NS & 5% RHA	2.16	2.50	2.73
3	1.0% NS & 10% RHA	2.70	2.96	3.28
4	1.5% NS & 15% RHA	2.34	2.71	3.07
5	2.0% NS & 20% RHA	2.03	2.35	2.66

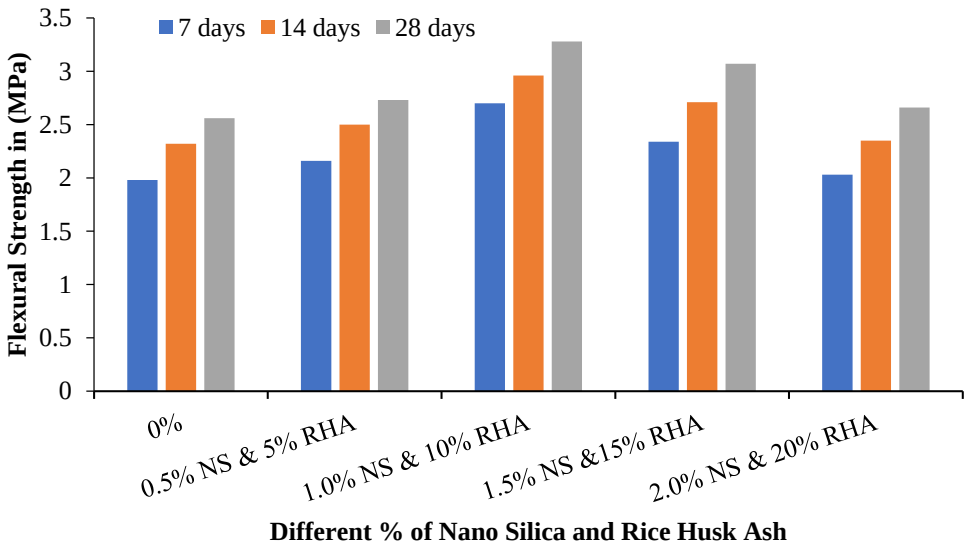

Figure 6. Split tensile strength of concrete with different proportions of NS and RHA.

3.4. Material Properties

A standardized 2D SEM image technique was implemented to measure the pore size distribution [47] and pore characteristics of materials [48,49]. The 2D morphological properties of concrete were determined using 2D projections. 3D morphological properties were obtained using reconstructed multiphysics models. The SEM images were captured using a JOEL scanning electron microscope (JSM-IT800). The image processing technique was adapted to analyze the percentages of air gaps, cement matrix, and aggregate distribution in the concrete. A series of 2D X-ray images are used to create 2D and 3D multiphysics model images. Images in 2D and 3D can be utilized to analyze a specimen's interior structure [47].

The specimen is rotated between an X-ray source and an X-ray detector on a rotating table. For each location of the revolving table, X-rays are transmitted through the specimen. Each slice gets 2D X-ray transmission images as a result of this. Special algorithms are used to rebuild the images of the slices, resulting in a 3D data set for the specimen structure. A deep mapping algorithm from MATLAB image processing toolbox was adopted. Image processing is a technique for implementing operations on an image in order to improve it or extract valuable information from it. It is a form of signal processing in which the input is an image, and the output is either that picture or its characteristics/features. Image processing converts an image into digital form and applies a procedure to it to obtain a better image or extract useful information. The first one is the enhancement of visual data for human interpretation, and the second one is scene data processing for autonomous machine perception. Such examination is one of the most popular non-destructive techniques to describe concrete microstructure without damaging the material. The first image on the top left position of Figures 7–9 show an original 2D SEM image [46–56] which allows the user to generate a binary image shown immediately on the right. This binary image represents the pore phase in the target component of this investigation. One of the main novelties of this study is the quantitative use of SEM images to detect and measure the size of concrete pore spaces using a watershed segmentation algorithm. The optimum dosage of NS 1.0% and RHA 10% [57,58] was chosen for this image processing.

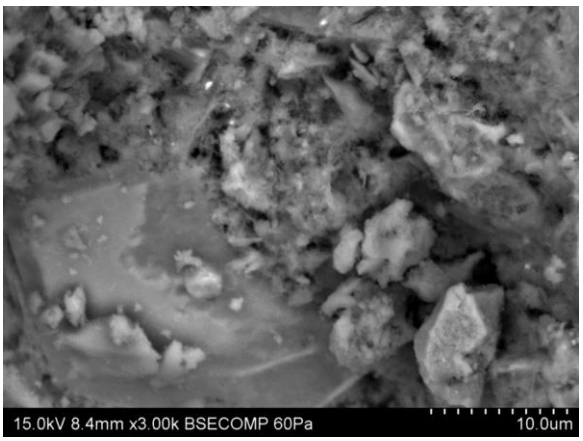

Original Image

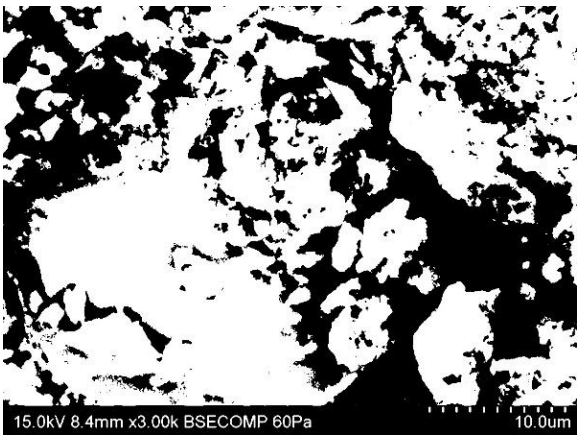

Binary Segmentation

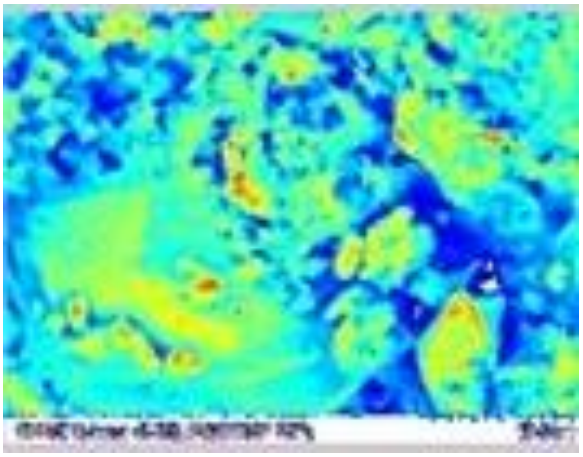

Deep Mapping

Pore Space Segmentation

Figure 7. *Cont.*

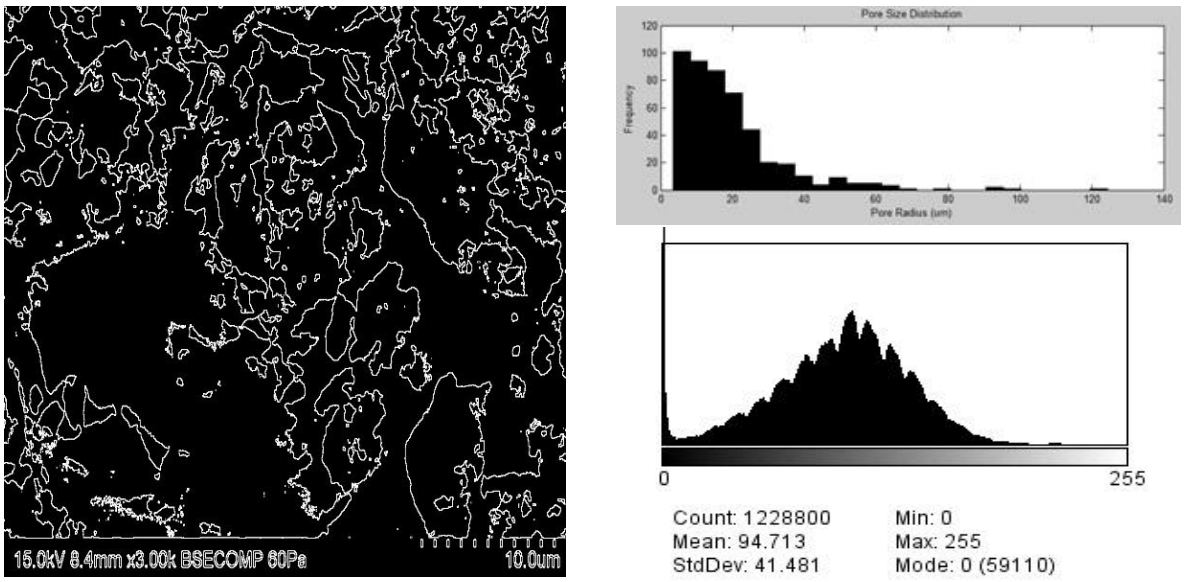

Figure 7. 2D SEM images of concrete microstructures.

The binary image consists of clustered pores that should be separated from the sample. A modified deep mapping algorithm was used to identify the clear pore segments. The next image on the right shows different colors denoting every single pore which generates the next pore size segmental image on the right. The pore space segmentation characterization is an important method to understand the mechanical properties of concrete [35,59–63]. Table 8 shows the output of MATLAB Analysis of different images of NS and RHA.

Image processing is a non-destructive technique that can be used for predicting the compressive strength of concrete with various applications in the construction sector. The

SEM image technique was used to analyze the concrete samples' binary segmentation and pore space segmentation. The grayscale images provide the edge formation in concrete. In the final step, the histogram identifies the points that are the graphical representation of image pixel values. Such interface image processing is used to determine the percentage of air space, aggregate, and cement distribution in the concrete [36,37,64–66].

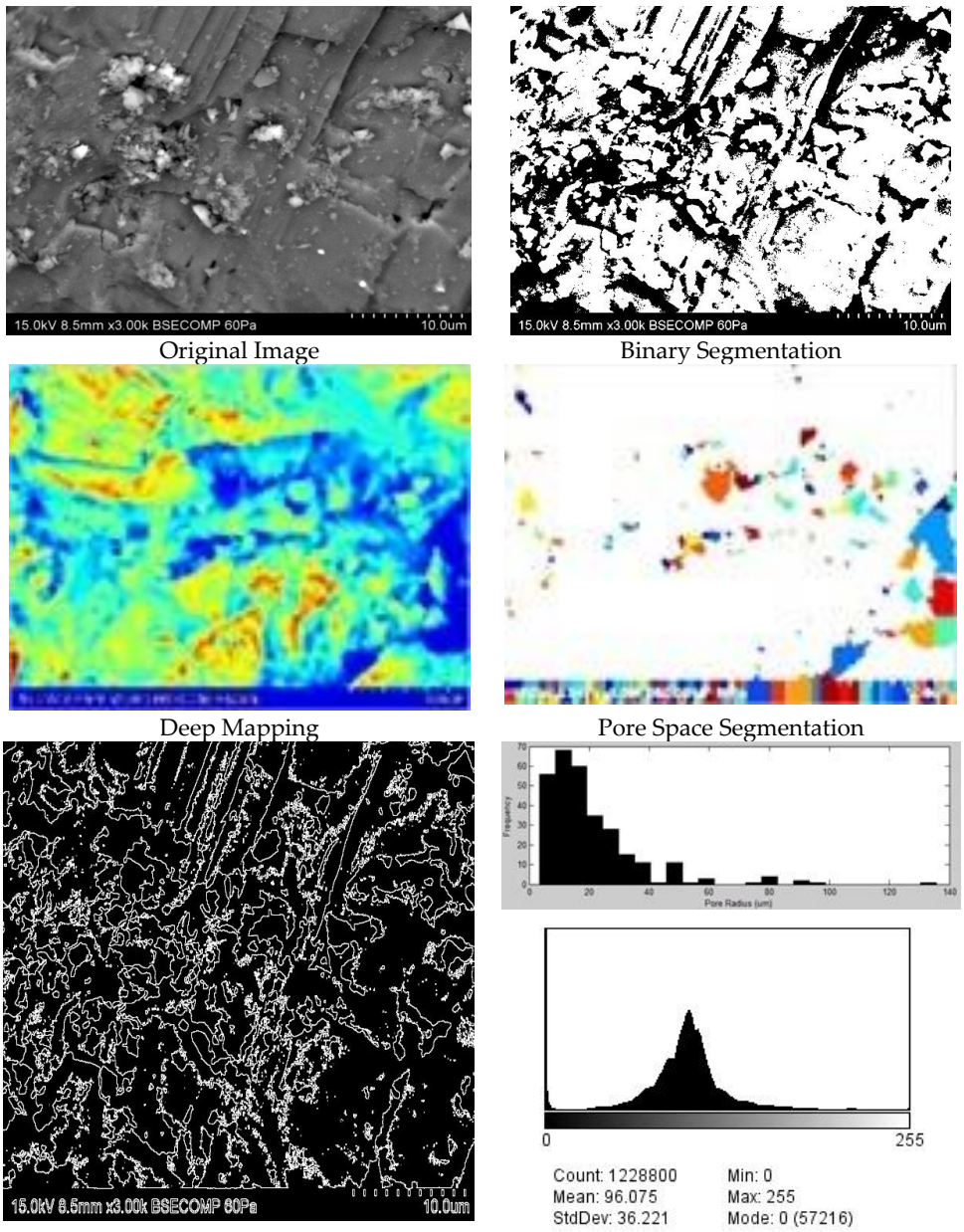

Figure 8. *Cont*.

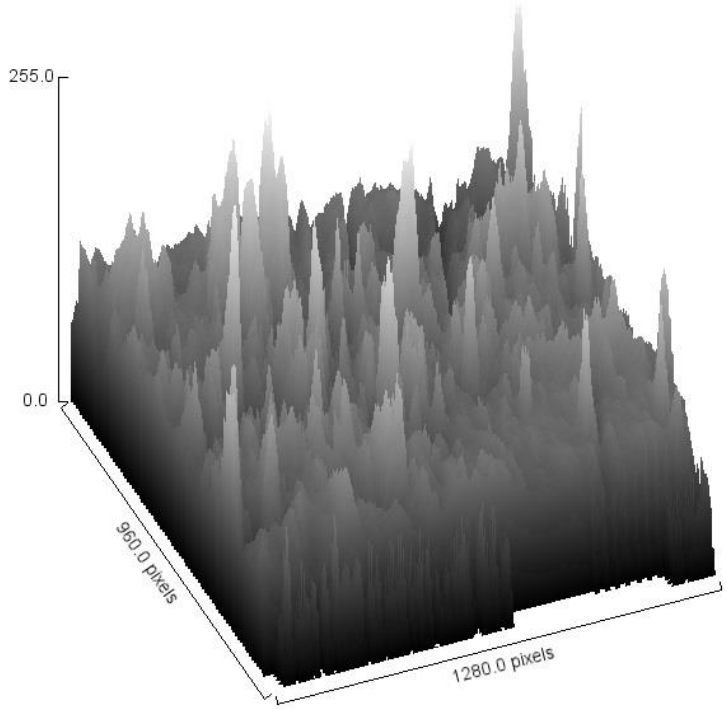

Figure 8. 2D SEM image processing of concrete microstructures.

Using the standard EN 480-11, the two-dimensional pore size distribution was determined. The scanning electron microscope was utilized to process the images without damaging the material properties. The gray color particles in the binary segmentation represent the pores in the sample. Therefore, special care was paid to the gray images. The measured porosity values are given in Figure 9. It can be observed that the average pore radius and cracking surface show consistency, which confirms the effectiveness and accuracy of the image processing technique. The measured areas tend to increase when the air gap increases for all the samples. The size distribution of each pore showed a similar pattern in different cases, and such measured distribution is compared using the image processing technique. The histogram image of the original SEM provides the distribution of intensity of each material. Various materials such as aggregates, cement portions, and air-voids in concrete make different noises [56,57]. However, the micro image shows a similar trend and better understanding.

There are air-voids, capillary pores, and gel pores in the pore microstructure of cement-based materials, and the pores are randomly sized, organized, and related to each other. Porosity is a well-known characteristic that affects strength and durability directly. As a matter of fact, a reduction in concrete porosity with adequate binding material content will contribute to increasing concrete strength [50–55]. In this experimental investigation and image processing, the same was adopted, such as samples A (concrete with RHA and without NS), B (concrete with RHA and sonicated NS), and C (concrete with RHA and unsonicated NS) have been analyzed with SEM techniques for predicting the properties of concrete incorporated with NS and RHA. Table 9 presents the results of image processing for the Sample A, B, and C.

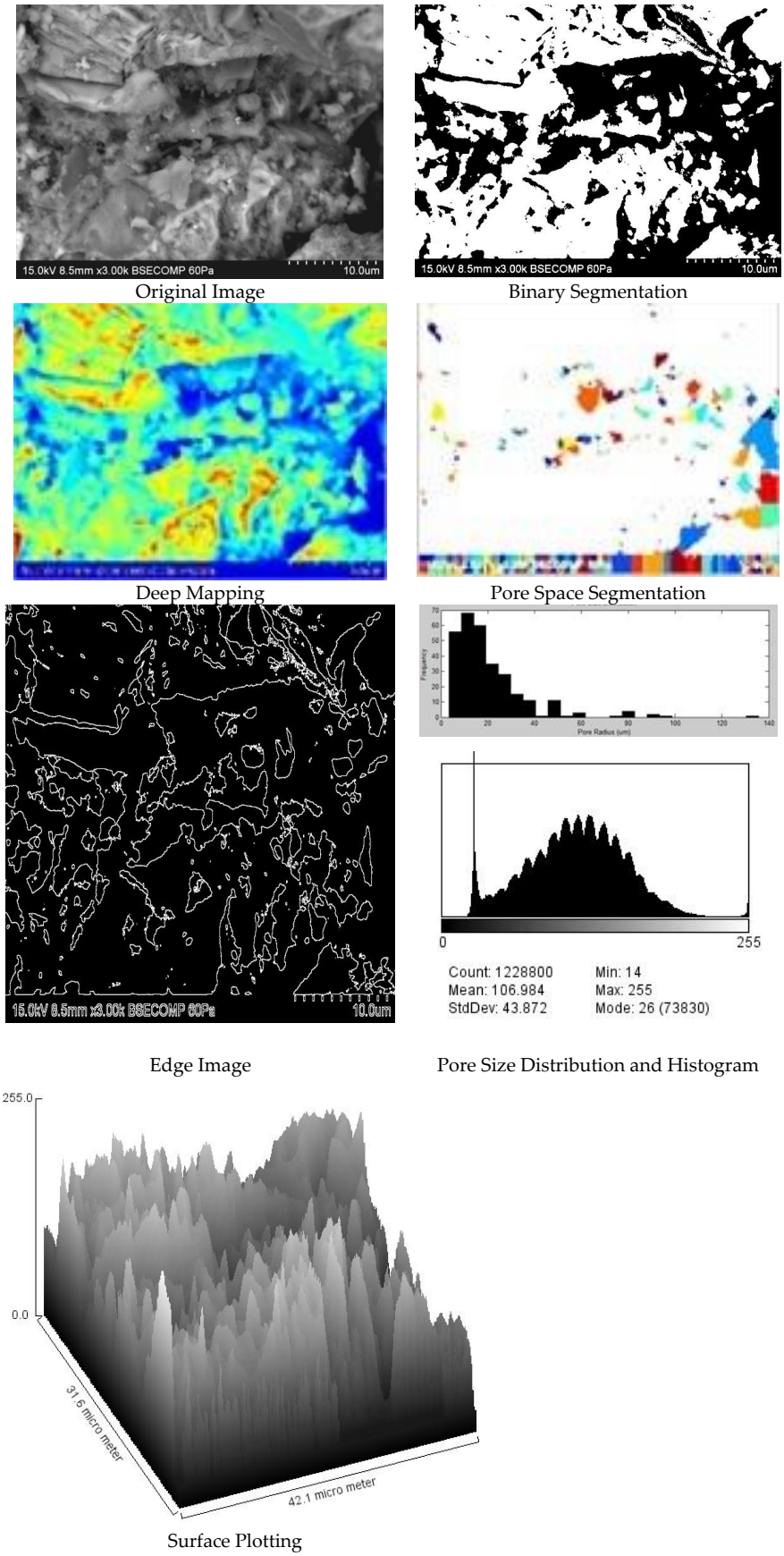

Figure 9. 2D SEM image processing of concrete microstructure.

Table 9. The output of MATLAB Analysis.

	Sample A	Sample B	Sample C
Porosity %	0.1784	0.0693	0.1397
Average pore radius (μm)	18.8447	17.0092	20.7707
Standard deviation of pore radius	14.7276	11.7858	16.9897

Sample A—(concrete with RHA and without NS), Sample B—(concrete with RHA and sonicated NS) and Sample C—(concrete with RHA and unsonicated NS) [46].

In general, pore microstructure affects the physical characteristics of engineering materials (such as strength, fracture energy and toughness, elastic properties, permeability, and efficient diffusivity) and environmental stability (such as durability and reliability) and is an important means of regulating the life expectancy and the cost-effectiveness of materials and structures. Table 9 presents the results obtained using MATLAB.

4. Conclusions

The conclusions of the present work are summarized in the following.

− NS added to cement as a supplementary component accelerates the heat of hydration and hydration degree of cement. Depending on the NS content, it significantly increases the water demand in the cement paste, which decreases the setting time compared to conventional concrete.
− NS lowers the water demand in the mixing process of concrete, delaying the setting times and reducing the heat of hydration generated in concrete. This is related to a reduction of the mechanical strength. The addition of NS and RHA influenced concrete workability. It can be observed that, with the rise in the percentage of NS and RHA, the workability decreased. The voids and porosity of concrete were minimized by incorporating the NS and RHA.
− When NS is added to the concrete mix, the amount of CSH gel formed in the matrix increases, which helps to fill the pores in concrete. Inactive NS also acts as a filler. Through these factors, NS minimizes pore volume and helps concrete to be well compacted. As a result, NS modify concrete is extremely durable.
− The mechanical qualities of concrete combined with RHA and NS have improved by up to 10% over the control mix. Due to its greater specific surface, particle sizes, and porous structure, the matrix contains SF, which absorbs a large quantity of moisture and leads to the creation of CSH. The RHA absorbs moisture, which reacts with Ca^{2+} ions in cementitious materials, enhancing the pozzolanic reaction and leading to concrete's early and long-term growth in compressive strength, splitting tensile, and flexural strength.
− When increasing NS and RHA content up to 1.0% and 10%, respectively, the compressive, flexural, and tensile strength at 28 days increased, respectively. Above 1.0% NS and 10% RHA content, strength decreased. It is suggested that 1.0% NS and 10% RHA are the optimum dosages to incorporate in concrete compared to the other NS- and RHA-based concrete. Furthermore, an increase of NS and RHA led to a decrease in the compressive strength of concrete.
− The microscopic test confirms that RHA particles collapse the porous structure during the grinding process, resulting in pore volume reduction. Direct or indirect sonication of NS improves the dispersion capacity of the cement matrix. Furthermore, when using direct sonication, NS is more homogenized rather than using indirect sonication.
− The gray tone threshold values of aggregate and cement can be used to predict the compressive strength of concrete using an image-processing tool.
− The 3D multiphysics model image can be effectively utilized for defining the pore size distribution. In addition, peaks represented by the large pore size were used to characterize materials.

− The proposed systematic evaluation process verifies the accuracy of predicting the pores of materials. Furthermore, the correlation between the compressive strength of concrete and pore size distribution confirms the cracking of materials.

The above findings reveal the potential of using NS and RHA in concrete to enhance its efficiency and strength. Other natural fibers can also be used to improve load transfer, compressive strength, flexural strength, and ductility in concrete. This will represent the subject of a future investigation. Furthermore, the continuation of this research is in progress to perform numerous experimental tests that focus on the TGA-DTG, FT-IR comparing the results before incorporating SN and RHA and after the incorporation.

Author Contributions: Conceptualization, S.A., S.P. and E.I.S.F.; Data curation, M.A., R.A., E.I.S.F., R.D., R.G., R.F. and N.V.; Formal analysis, S.A., S.P., M.A., R.A., E.I.S.F., R.D., R.G., R.F. and N.V.; Funding acquisition, M.A., R.F. and N.V.; Investigation, S.A. and S.P.; Methodology, S.P.; Project administration, M.A., R.A. and E.I.S.F.; Resources, R.D. and N.V.; Software, R.G. and R.F.; Validation, S.P., M.A., R.A., E.I.S.F., R.F. and N.V.; Visualization, R.D. and R.G.; Writing—original draft, S.A., S.P. and R.A.; Writing—review & editing, M.A., E.I.S.F., R.D., R.G., R.F. and N.V. All authors have read and agreed to the published version of the manuscript.

Funding: The research is partially funded by the Ministry of Science and Higher Education of the Russian Federation as part of the World-class Research Center program: Advanced Digital Technologies (contract No. 075-15-2020-934 dated 17 November 2020).

Institutional Review Board Statement: Not applicable.

Informed Consent Statement: Not applicable.

Data Availability Statement: Not applicable.

Acknowledgments: S.A. and E.I.S.F. acknowledge funding coming from the Universidad de Santiago de Chile, Usach, Proyecto POSTDOC_DICYT, Código 052018SF_POSTDOC, Vicerrectoría de Investigación, Desarrollo e Innovación. Also, the authors gratefully acknowledge the financial support given by the Deanship of Scientific Research at Prince Sattam bin Abdulaziz University, Alkharj, Saudi Arabia; and the Peter the Great Polytechnic University, Saint Petersburg, Russia, and cooperation of the Department of Civil Engineering, Faculty of Engineering and IT, Amran University, Yemen, for this research.

Conflicts of Interest: The authors declare no conflict of interest.

References

1. Zahedi, M.; Ramezanianpour, A.A.; Ramezanianpour, A.M. Evaluation of the mechanical properties and durability of cement mortars containing Nano silica and rice husk ash under chloride ion penetration. *Constr. Build. Mater.* **2015**, *78*, 354–361. [CrossRef]
2. Ganesan, K.; Rajagopal, K.; Thangavel, K. Rice Husk Ash blended cement assessment of optimal level of replacement for strength and permeability of concrete. *Constr. Build. Mater.* **2008**, *22*, 1675–1683. [CrossRef]
3. Rai, S.; Tiwari, S. Nano Silica in Cement Hydration. *Mater. Today Proc.* **2018**, *5*, 9196–9202. [CrossRef]
4. Magar, R.B.; Khan, A.; Gupta, V.; Gupta, V.; Sayed, K. Effect of Colloidal Nano silica on High Strength Rice Husk Ash Concrete. *Int. J. Concr. Technol.* **2017**, *3*, 1–11.
5. Amran, M.; Fediuk, R.; Murali, G.; Vatin, N.; Karelina, M.; Ozbakkaloglu, T.; Krishna, R.S.; Kumar, S.A.; Kumar, D.S.; Mishra, J. Rice husk ash-based concrete composites: A critical review of their properties and applications. *Crystals* **2021**, *11*, 168. [CrossRef]
6. Prasada Rao, D.V.; Nvaneethamma, V. Influence of Nano-Silica on Strength Properties of Concrete Containing Rice Husk Ash. *Int. J. Adv. Res. Educ. Amp. Technol.* **2016**, *3*, 39–43.
7. Givi, A.N.; Rashid, S.A.; Aziz, F.N.A.; Salleh, M.A.M. Assessment of the effects of rice husk ash particle size on strength water permeability and workability of binary blended concrete. *Constr. Build. Mater.* **2010**, *24*, 2145–2150. [CrossRef]
8. Ji, T. Preliminary study on the water permeability & amp; microstructure of concrete incorporating nano-SiO_2. *Cem. Concr. Res.* **2005**, *35*, 1943–1947.
9. Mohan, R.B.; Sugila, D.V. Experimental investigation on Nano concrete with Nano silica and m-sand. *Int. Res. J. Eng. Technol.* **2019**, *6*, 6860–6871.
10. Torabian Isfahani, F.; Redaelli, E.; Lollini, F.; Li, W.; Bertolini, L. Effects of Nanosilica on Compressive Strength and Durability Properties of Concrete with Different Water to Binder Ratios. *Adv. Mater. Sci. Eng.* **2016**, *2016*, 1–16. [CrossRef]

11. Chotard, T.J.; Boncoeur-Martel, M.P.; Smith, A.; Dupuy, J.P.; Gault, C. Application of X-ray computed tomography to characterise the early hydration of calcium aluminate cement. *Cem. Concr. Compos.* **2003**, *25*, 145–152. [CrossRef]
12. Natesaiyer, K.; Chan, C.; Sinha-Ray, S.; Song, D.; Lin, C.L.; Miller, J.D.; Garboczi, E.J.; Forster, A.M. X-ray CT imaging and finite element computations of the elastic properties of a rigid organic foam compared to experimental measurements: Insights into foam variability. *J. Mater. Sci.* **2015**, *50*, 4012–4024. [CrossRef]
13. Nagataki, S.; Fujiwara, H. *Self-Compacting Property of Highlyflowable Concrete*; Special Publication; ACI: Farmington Hills, MI, USA, 1995; Volume 154, pp. 301–304.
14. Björnström, J.; Martinelli, A.; Matic, A.; Börjesson, L.; Panas, I. Accelerating effects of colloidal nano-silica for beneficial calcium silicate hydrate formation in cement. *Chem. Phys. Lett.* **2004**, *392*, 242–248. [CrossRef]
15. Amran, M.; Fediuk, R.; Murali, G.; Vatin, N.; Al-Fakih, A. Sound-Absorbing Acoustic Concretes: A Review. *Sustainability* **2021**, *13*, 10712. [CrossRef]
16. Jo, B.W.; Kim, C.H.; Lim, J.H. Investigations on the development of powder concrete with nano-SiO particles. *KSCE J. Civ. Eng.* **2007**, *11*, 37–42. [CrossRef]
17. Supit, M.S.W.; Shaikh, F.U.A. Durability properties of high volume fly ash concrete containing nano-silica. *Mater. Struct.* **2015**, *48*, 2431–2445. [CrossRef]
18. Rezania, M.; Panahandeh, M.; Razavi, S.M.J.; Berto, F. Experimental study of the simultaneous effect of nano-silica and nano-carbon black on permeability and mechanical properties of the concrete. *Theor. Appl. Fract. Mech.* **2019**, *104*, 102391. [CrossRef]
19. Khatri, R.P.; Sirivivatnanon, V.; Gross, W. Effect of different supplementary cementitious materials on mechanical properties of high performance concrete. *Cem. Concr. Res.* **1995**, *25*, 209220. [CrossRef]
20. Mazloom, M.; Ramezanianpour, A.A.; Brooks, J.J. Effect of silica fume on mechanical properties of high-strength concrete. *Cem. Concr. Compos.* **2004**, *26*, 347–357. [CrossRef]
21. Beigi, M.H.; Berenjian, J.; Omran, O.L.; Nik, A.S.; Nikbin, I.M. An experimental survey on combined effects of fibers and nanosilica on the mechanical, rheological, and durability properties of self compacting concrete. *Mater. Des.* **2013**, *50*, 1019–1029. [CrossRef]
22. Rong, Z.D.; Sun, W.; Xiao, H.J.; Jiang, G. Effects of nano-SiO particles on the mechanical and microstructural properties of ultrahigh performance cementitious composites. *Cem. Concr. Compos.* **2015**, *56*, 25–31. [CrossRef]
23. Givi, A.N.; Rashid, S.A.; Aziz, F.N.A.; Salleh, M.A.M. Experimental investigation of the size effects of SiO_2 nano-particles on the mechanical properties of binary blended concrete. *Compos. Part B Eng.* **2010**, *41*, 673–677. [CrossRef]
24. Amran, M.; Debbarma, S.; Ozbakkaloglu, T. Fly ash-based eco-friendly geopolymer concrete: A critical review of the long-term durability properties. *Constr. Build. Mater.* **2021**, *270*, 121857. [CrossRef]
25. Abdellahi, M.; Karafshani, M.K.; Rizi, A.S. Modeling effect of SiO_2 nanoparticles on the mechanical properties of the concretes. *J. Build. Pathol. Rehabil.* **2017**, *2*, 8. [CrossRef]
26. Khaloo, A.; Mobini, M.H.; Hosseini, P. Influence of different types of nano-SiO particles on properties of high-performance concrete. *Constr. Build. Mater.* **2016**, *113*, 188–201. [CrossRef]
27. Horszczaruk, E.; Sikora, P.; Cendrowski, K.; Mijowska, E. The effect of elevated temperature on the properties of cement mortars containing nanosilica and heavyweight aggregates. *Constr. Build. Mater.* **2017**, *137*, 420–431. [CrossRef]
28. Wang, X.F.; Huang, Y.J.; Wu, G.Y.; Fang, C.; Li, D.W.; Han, N.X.; Xing, F. Effect of nano-SiO on strength, shrinkage and cracking sensitivity of lightweight aggregate concrete. *Constr. Build. Mater.* **2018**, *175*, 115–125. [CrossRef]
29. Heidari, A.; Tavakoli, D. A study of the mechanical properties of ground ceramic powder concrete incorporating nano-SiO_2 particles. *Constr. Build. Mater.* **2013**, *38*, 255–264. [CrossRef]
30. Ibrahim, M.; Johari, M.A.M.; Maslehuddin, M.; Rahman, M.K. Influence of nano-SiO on the strength and microstructure of natural pozzolan based alkali activated concrete. *Constr. Build. Mater.* **2018**, *173*, 573–585. [CrossRef]
31. Ltifi, M.; Guefrech, A.; Mounanga, P.; Khelidj, A. Experimental study of the effect of addition of nano-silica on the behaviour of cement mortars. *Procedia Eng.* **2011**, *10*, 900–905. [CrossRef]
32. Onaizi, A.M.; Huseien, G.F.; Lim, N.H.; Amran, M.; Samadi, M. Effect of nanomaterials inclusion on sustainability of cement-based concretes: A comprehensive review. *Constr. Build. Mater.* **2021**, *306*, 124850. [CrossRef]
33. Fallah, S.; Nematzadeh, M. Mechanical properties and durability of high-strength concrete containing macro-polymeric and polypropylene fibers with nano-silica and silica fume. *Constr. Build. Mater.* **2017**, *132*, 170–187. [CrossRef]
34. Nili, M.; Ehsani, A. Investigating the effect of the cement paste and transition zone on strength development of concrete containing nanosilica and silica fume. *Mater. Des.* **2015**, *75*, 174–183. [CrossRef]
35. Al-Rousan, T.; Masad, E.; Tutumluer, E.; Tongyan, P. Evaluation of image analysis techniques for quantifying aggregate shape characteristics. *J. Constr. Build. Mater.* **2007**, *21*, 978–990. [CrossRef]
36. Başyiğit, C.; Comak, B.; Kılınçarslan, Ş.; Üncü, I.S. Assessment of concrete compressive strength by image processing technique. *Constr. Build. Mater.* **2012**, *37*, 526–532. [CrossRef]
37. Zelelew, H.M.; Almuntashri, A.; Agaian, S.; Papagiannakis, A.T. An improved image processing technique for asphalt concrete X-ray CT images. *Road Mater. Pavement Des.* **2013**, *14*, 341–359. [CrossRef]
38. Brescia-Norambuena, L.; González, M.; Avudaiappan, S.; Flores, E.I.S.; Grasley, Z. Improving concrete underground mining pavements performance through the synergic effect of silica fume, nanosilica, and polypropylene fibers. *Constr. Build. Mater.* **2021**, *285*, 122895. [CrossRef]

39. Bureau of Indian Standards. *Indian Standards IS: 2386 (Part-1), Methods of Test for Aggregates for Concrete: Particle Size and Shape*; Bureau of Indian Standards: New Delhi, India, 1963.
40. Arularasi, V.; Thamilselvi, P.; Avudaiappan, S.; Saavedra Flores, E.I.; Amran, M.; Fediuk, R.; Vatin, N.; Karelina, M. Rheological Behavior and Strength Characteristics of Cement Paste and Mortar with Fly Ash and GGBS Admixtures. *Sustainability* **2021**, *13*, 9600. [CrossRef]
41. Bureau of Indian Standards. *Indian Standards IS: 1199-1959, Methods of Sampling and Analysis of Concrete*; Bureau of Indian Standards: New Delhi, India, 1959.
42. Bureau of Indian Standards. *Indian Standards IS: 516-1959, Method of Tests for Strength of Concrete*; Bureau of Indian Standards: New Delhi, India, 2004.
43. Bureau of Indian Standards. *Indian Standards IS: 5816-1999, Method of Tests for Splitting Tensile Strength of Concrete*; Bureau of Indian Standards: New Delhi, India, 1999.
44. Bureau of Indian Standards. *Indian Standards IS: 269-1989, Specification for 33 Grade Ordinary Portland Cement*; Bureau of Indian Standards: New Delhi, India, 2015.
45. Amran, M.; Fediuk, R.; Murali, G.; Avudaiappan, S.; Ozbakkaloglu, T.; Vatin, N.; Karelina, M.; Klyuev, S.; Gholampour, A. Fly ash-based eco-efficient concretes: A comprehensive review of the short-term properties. *Materials* **2021**, *14*, 4264. [CrossRef]
46. Sharobim, K.G.; Mohamadien, H.A.; Hanna, N.F.; El-Feky, M.S.; Khattab, E.; El-Tair, A.M. Optimizing sonication time and solid to liquid ratio of nano-silica in high strength mortars. *Int. J. Curr. Trends Eng. Res.* **2017**, *3*, 6–16.
47. Chung, S.Y.; Sikora, P.; Rucinska, T.; Stephan, D.; Abd Elrahman, M. Comparison of the pore size distributions of concretes with different airentraining admixture dosages using 2D and 3D imaging approaches. *Mater. Charact.* **2020**, *162*, 110182. [CrossRef]
48. Neithalath, N.; Sumanasooriya, M.S.; Deo, O. Characterizing pore volume, size, and connectivity in pervious concretes for permeability prediction. *Mater. Charact.* **2010**, *61*, 802–813. [CrossRef]
49. Bossa, N.; Chaurand, P.; Vicente, J.; Borschneck, D.; Levard, C.; Aguerre-Chariol, O.; Rose, J. Micro- and nano-X-ray computed-tomography: A step forward in the characterization of the pore-network of a leached cement paste. *Cem. Concr. Res.* **2015**, *67*, 138–147. [CrossRef]
50. Kim, K.Y.; Yun, T.S.; Choo, J.; Kang, D.H.; Shin, H.S. Determination of air-void parameters of hardened cement-based materials using X-ray computed tomography. *Constr. Build. Mater.* **2012**, *37*, 93–101. [CrossRef]
51. Da Silva, Í.B. X-ray Computed Microtomography technique applied for cementitious materials: A review. *Micron* **2018**, *107*, 1–8. [CrossRef] [PubMed]
52. Onaizi, A.M.; Lim, N.H.; Huseien, G.F.; Amran, M.; Ma, C.K. Effect of the addition of nano glass powder on the compressive strength of high volume fly ash modified concrete. *Mater. Today Proc.* **2021**, 975–983.
53. Lu, H.; Peterson, K.; Chernoloz, O. Measurement of entrained air-void parameters in Portland cement concrete using micro X-ray computed tomography. *Int. J. Pavement Eng.* **2016**, *19*, 109–121. [CrossRef]
54. Chung, S.-Y.; Lehmann, C.; Abd Elrahman, M.; Stephan, D. Pore characteristics and their effects on the material properties of foamed concrete evaluated using micro-CT images and numerical approaches. *Appl. Sci.* **2017**, *7*, 550. [CrossRef]
55. Al-hokabi, A.; Hasan, M.; Amran, M.; Fediuk, R.; Vatin, N.I.; Klyuev, S. Improving the Early Properties of Treated Soft Kaolin Clay with Palm Oil Fuel Ash and Gypsum. *Sustainability* **2021**, *13*, 10910. [CrossRef]
56. Joshi, S.K. On application of image processing: Study of digital image processing techniques for concrete mixture images and its composition. *Int. J. Eng. Res. Technol.* **2014**, *3*, 1137–1146.
57. Amran, M.; Al-Fakih, A.; Chu, S.H.; Fediuk, R.; Haruna, S.; Azevedo, A.; Vatin, N. Long-term durability properties of geopolymer concrete: An in-depth review. *Case Stud. Constr. Mater.* **2021**, *15*, e00661.
58. Givi, A.N.; Rashid, S.A.; Aziz, F.N.A.; Salleh, M.A.M. Influence of 15 and 80 nano-SiO_2 particles addition on mechanical and physical properties of ternary blended concrete incorporating rice husk ash. *J. Exp. Nanosci.* **2013**, *8*, 1–18. [CrossRef]
59. Noaman, M.A.; Karim, M.R.; Islam, M.N. Comparative study of pozzolanic and filler effect of rice husk ash on the mechanical properties and microstructure of brick aggregate concrete. *Heliyon* **2019**, *5*, e01926. [CrossRef] [PubMed]
60. Lesovik, V.; Fediuk, R.; Amran, M.; Vatin, N.; Timokhin, R. Self-Healing Construction Materials: The Geomimetic Approach. *Sustainability* **2021**, *13*, 9033. [CrossRef]
61. Zhao, H.; Xiao, Q.; Huang, D.; Zhang, S. Influence of Pore Structure on Compressive Strength of Cement Mortar. *Sci. World J.* **2014**, *2014*, 247058. [CrossRef] [PubMed]
62. Kumar, R.; Bhattacharjee, B. Porosity, pore size distribution and in situ strength of concrete. *Cem. Concr. Res.* **2003**, *33*, 155–164. [CrossRef]
63. Muthusamy Kavitha, S.; Venkatesan, G.; Avudaiappan, S.; Saavedra Flores, E.I. Mechanical and flexural performance of self compacting concrete with natural fiber. *Rev. Constr. J. Constr.* **2020**, *19*, 370–380. [CrossRef]
64. Tran, H.B.; Le, V.B.; Phan, V.T.A. Mechanical Properties of High Strength Concrete Containing Nano SiO_2 Made from Rice Husk Ash in Southern Vietnam. *Crystals* **2021**, *11*, 932. [CrossRef]
65. Zhang, P.; Ling, Y.; Wang, J.; Shi, Y. Bending resistance of PVA fiber reinforced cementitious composites containing nano-SiO_2. *Nanotechnol. Rev.* **2019**, *8*, 690–698. [CrossRef]
66. Rajasegar, M.; Kumaar, C.M. Hybrid effect of poly vinyl alcohol, expansive minerals, nano-silica and rice husk ash on the self-healing ability of concrete. *Mater. Today Proc.* **2020**, *45*, 5944–5952. [CrossRef]